Supra-barrel Distribution of Directional Tuning for Global Motion in the Mouse Somatosensory Cortex

Maria Eugenia Vilarchao, Luc Estebanez, Daniel E. Shulz, Isabelle Ferezou

Article

Cell Reports

Supra-barrel Distribution of Directional Tuning for Global Motion in the Mouse Somatosensory Cortex

Graphical Abstract

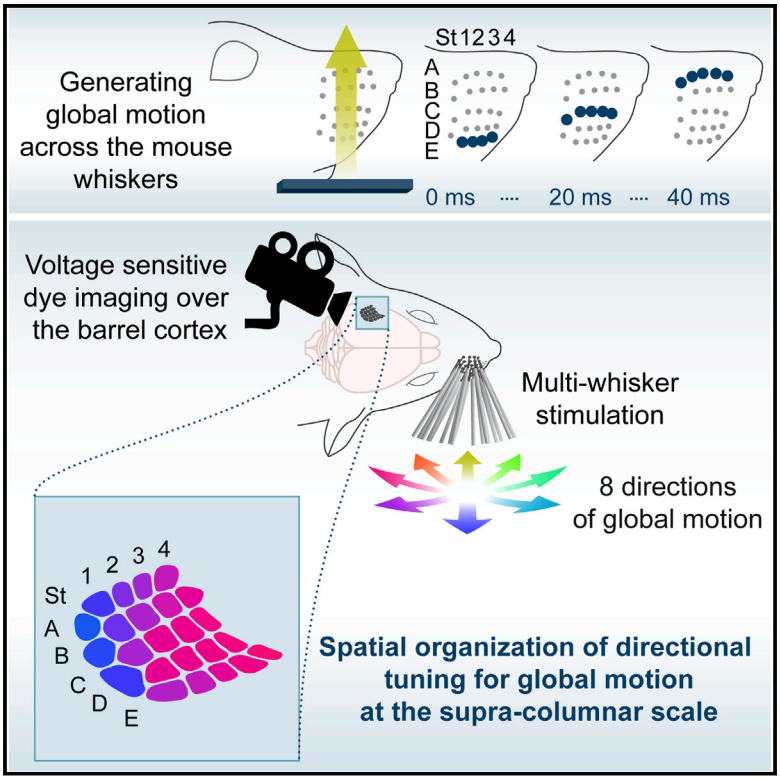

Highlights

- Multi-whisker stimuli generating global motions activate the entire barrel cortex
- Responses are sublinear and depend upon the direction of the global motion
- Overall, the barrel cortex responds preferentially to caudo-ventral global motions
- Directional tuning for global motion varies gradually over the barrel map

Authors

María Eugenia Vilarchao, Luc Estebanez, Daniel E. Shulz, Isabelle Férézou

Correspondence

daniel.shulz@unic.cnrs-gif.fr (D.E.S.), isabelle.ferezou@unic.cnrs-gif.fr (I.F.)

In Brief

Using voltage-sensitive dye imaging of the mouse barrel cortex, Vilarchao et al. demonstrate the presence of direction selectivity to global motion generated by multi-whisker stimuli. Selectivity to global motion is spatially organized at the supra-columnar scale with an overrepresentation of selectivity to caudo-ventral directions.

Vilarchao et al., 2018, Cell Reports *22*, 3534–3547
March 27, 2018
https://doi.org/10.1016/j.celrep.2018.03.006

CellPress

OPEN ACCESS
CellPress

Cell Reports
Article

Supra-barrel Distribution of Directional Tuning for Global Motion in the Mouse Somatosensory Cortex

María Eugenia Vilarchao,[1,2] Luc Estebanez,[1] Daniel E. Shulz,[1,*] and Isabelle Férézou[1,3,*]
[1]Unité de Neurosciences, Information et Complexité, Centre National de la Recherche Scientifique, FRE 3693, 91198 Gif-sur-Yvette, France
[2]Present address: Laboratory for Perception and Memory, Institut Pasteur and Centre National de la Recherche Scientifique, UMR 3571, 75015 Paris, France
[3]Lead Contact
*Correspondence: daniel.shulz@unic.cnrs-gif.fr (D.E.S.), isabelle.ferezou@unic.cnrs-gif.fr (I.F.)
https://doi.org/10.1016/j.celrep.2018.03.006

SUMMARY

Rodents explore their environment with an array of whiskers, inducing complex patterns of whisker deflections. Cortical neuronal networks can extract global properties of tactile scenes. In the primary somatosensory cortex, the information relative to the global direction of a spatiotemporal sequence of whisker deflections can be extracted at the single neuron level. To further understand how the cortical network integrates multi-whisker inputs, we imaged and recorded the mouse barrel cortex activity evoked by sequences of multi-whisker deflections generating global motions in different directions. A majority of barrel-related cortical columns show a direction preference for global motions with an overall preference for caudo-ventral directions. Responses to global motions being highly sublinear, the identity of the first deflected whiskers is highly salient but does not seem to determine the global direction preference. Our results further demonstrate that the global direction preference is spatially organized throughout the barrel cortex at a supra-columnar scale.

INTRODUCTION

Layer 4 of the rodent primary somatosensory cortex contains anatomical structures named ''barrels'' topologically organized as the whiskers on the animal's snout. Since their description by Woolsey and Van der Loos (1970), the barrels are considered as the prototypical morphological manifestation of the functional columnar organization of the cerebral cortex. Each neuronal column associated with a barrel processes primarily the information coming from its corresponding whisker (Feldmeyer et al., 2013; Petersen, 2003, 2007). However, when rodents explore their environment, they contact objects with the whole array of whiskers, inducing complex sequences of multi-whisker deflections. Although the topographic organization of the whisker-to-barrel cortex pathway suggests a parallel processing of the inputs originating from distinct whiskers, it also contains the neural bases for the integration of more complex interwhisker information (Armstrong-James and Callahan, 1991; Arnold et al., 2001; Ego-Stengel et al., 2005; Narayanan et al., 2015).

The principal candidates for integrating complex spatiotemporal sequences of tactile inputs are neurons with multi-whisker receptive fields (RFs). It has been shown that, in the supra- and infragranular layers of the barrel cortex, single neurons receive inputs from their principal whisker (PW) and from several surrounding whiskers (Brecht and Sakmann, 2002; Brecht et al., 2003; Manns et al., 2004; Moore and Nelson, 1998; Zhu and Connors, 1999). The structure of these multi-whisker RFs is stimulus dependent. They differ according to the direction of the whisker deflection (Le Cam et al., 2011). In addition to multi-whisker thalamic input, the cortico-cortical connections have profound effects on the RFs and the spread of subthreshold activity. For example, intracortical circuitry shows anisotropy toward within-row connectivity (Kim and Ebner, 1999; Petersen and Sakmann, 2001; Simons, 1978). A morphometric study revealed a much higher degree of horizontal connectivity than originally reported in the rat barrel cortex, with a majority of excitatory neurons projecting their axon far beyond their cortical column (Narayanan et al., 2015). Altogether, these observations suggest that complex interactions are likely to take place in the barrel cortex and might be essential for the integration of multi-whisker contacts.

Understanding how the barrel cortex can extract the emergent properties of such complex tactile inputs requires the use of multi-whisker stimuli that are locally invariant but differ by their global coherent properties. This is the case of ''global motion'' stimuli (Jacob et al., 2008), which consist in sequences of 24 whisker deflections presented in spatio-temporal orders mimicking front edges crossing the whisker pad in eight different directions. Single-unit recordings from the C2 barrel-related column in rat barrel cortex have shown that a majority of neurons are able to extract directional information from global motions independently of the local direction of deflections of individual whiskers. Preferred direction for global motions in regular spiking units presented a bias for caudo-ventral directions in the C2 barrel-related column (Jacob et al., 2008).

Whereas the spatial mapping of stimulus features, like the direction of a local stimulation, has been documented in the

visual and somatosensory cortices (Hubel and Wiesel, 1963; Andermann and Moore, 2006; Kremer et al., 2011), there is no experimental evidence for a spatial organization of global properties of stimulation at a larger spatial scale. Here, we hypothesized that directional tuning for global motion could be spatially distributed over the entire barrel cortex. Indeed, different dimensions of a stimulus can be mapped over the same cortical area. For instance, in cat visual cortex, the retinotopic, the ocular dominance, and the orientation selectivity maps are overlaid in the same cortical area (Hübener et al., 1997; Rothschild and Mizrahi, 2015). Evidence that multiple features of a stimulus can be represented within the same cortical area has been reported in the rat barrel cortex, where the somatotopic map coexists with a subcolumnar spatial mapping of direction preference for the individual deflection of the PW (Andermann and Moore, 2006; Kremer et al., 2011; Wilson et al., 2010).

Here, we assessed the spatial organization for the direction selectivity to global motions by means of voltage-sensitive dye (VSD) imaging and extracellular electrophysiological recordings of the cortical spatiotemporal dynamics evoked by multi-whisker stimuli.

RESULTS

VSD Imaging of Depolarizing Responses Evoked by Multi-whisker Stimuli

A mechanical multi-whisker stimulator (Jacob et al., 2010) was used to deflect the 24 macrovibrissae on the right side of the snout while recording the spatiotemporal dynamics of activity of the left barrel cortex by means of VSD imaging (Figure 1A). Multi-whisker stimuli were locally invariant—caudal or rostral whisker deflections—and globally coherent (Figure 1B), mimicking a bar moving in eight different directions, henceforth, "global directions." The whisker local deflection consisted of a 2.7° displacement with a 2-ms rising ramp, 2-ms plateau, and 2-ms fall (Figure 1C). The anatomical map of the layer 4 barrels was reconstructed post hoc (Perronnet et al., 2016; Supplemental Experimental Procedures) and superimposed to the functional VSD images using the surface blood vessels as anatomical landmarks.

A rostral global motion evoked a cortical activation that was initiated in the cortical columns corresponding to the first stimulated whiskers and then rapidly spread to cover the entire barrel cortex (Figure 1D). The cortical columns corresponding to the subsequently stimulated whiskers were activated even before the actual deflection of their corresponding whiskers. Measuring the signal from a region of interest (ROI) corresponding to the central C2 column indeed reveals that, at time 0, which corresponds to the actual deflection of the C2 whisker, a high level of activity is already present (46.83% of the peak response amplitude in this case). The response reaches its maximum 10 ms after the deflection of the arc 2 whiskers and slowly goes back to the baseline level. In addition to the activation of the whole barrel subfield, the global motion evoked the activation of a lateral area corresponding to the location of the secondary somatosensory cortex (Carvell and Simons, 1986).

The Evoked Responses Depend upon the Global Direction of the Multi-whisker Stimulation

Different global directions of stimulation elicited different patterns of responses. Figure 2A shows, for the same case as in Figure 1, the averaged response to eight global directions at different times relative to the stimulation of the central C2 whisker. For each direction, the early response occurred at regions representing the first stimulated whiskers. Subsequently, the activation spread across the barrel field according to the direction of the global motion. Finally, the late dynamics of the evoked cortical activity shared similar spatial properties.

For the eight global directions, the whiskers were always deflected in the same direction (either rostral or caudal); only the spatiotemporal sequence of the whisker deflections varied. If the cortex could extract global information about this spatiotemporal sequence, we could obtain, for a given cortical column, different responses to different global directions. To address this question, we first focused on the C2 column because of the central position of the C2 whisker in the stimulation matrix. The profiles of fluorescence computed from a ROI delimited by the anatomical C2 barrel are shown in Figure 2B, color coded for the eight directions of stimulation (same case as in Figures 1 and 2A). For all the global directions, the evoked activity reaches the C2 column before the whisker C2 was actually deflected (dashed line).

To quantify the degree of activity at the time of stimulation of the C2 whisker (T_0), we computed the level of activation relative to the maximum of the response for the eight directions and eight independent experiments (Figure 2C, top). All global directions showed an activation of the C2 barrel column around 50% at T_0 (52.55% ± 8.00%), except the global directions 45° and 90°, which showed lower activation (18.08% ± 0.24%). This fast lateral spread of activity is likely to impact the cortical activation induced by the C2 whisker deflection.

This suggests that, for most directions, the feedforward activity corresponding to the C2 whisker deflection contributes to only about half of the total amplitude of the response in the C2 column.

When measuring the responses latency in the C2 column, similar results were observed (Figure 2C, middle). For almost all directions, the latencies were negative, suggesting that the lateral spread of activity in the barrel cortex is faster than the moving bar stimulation on the receptive surface. As a consequence, if an adjacent row/arc was deflected 10 ms earlier, afferent signals coming from the thalamus might encounter neurons that were already activated by cortico-cortical connections, significantly impacting their responses. The shortest latencies correspond to the global motion of 315°, a direction that showed the smallest response (Figure 2C, bottom), suggesting that, within this global direction, the intracortical lateral connections might have a more prominent impact on the feedforward responses to the C2 whisker deflection.

The velocity of the cortical propagation of the early activation evoked by global motions was further quantified by focusing on the 4 cardinal directions (0°, 90°, 180°, and 270°), where the initial front edge of the stimulus similarly involves the synchronous

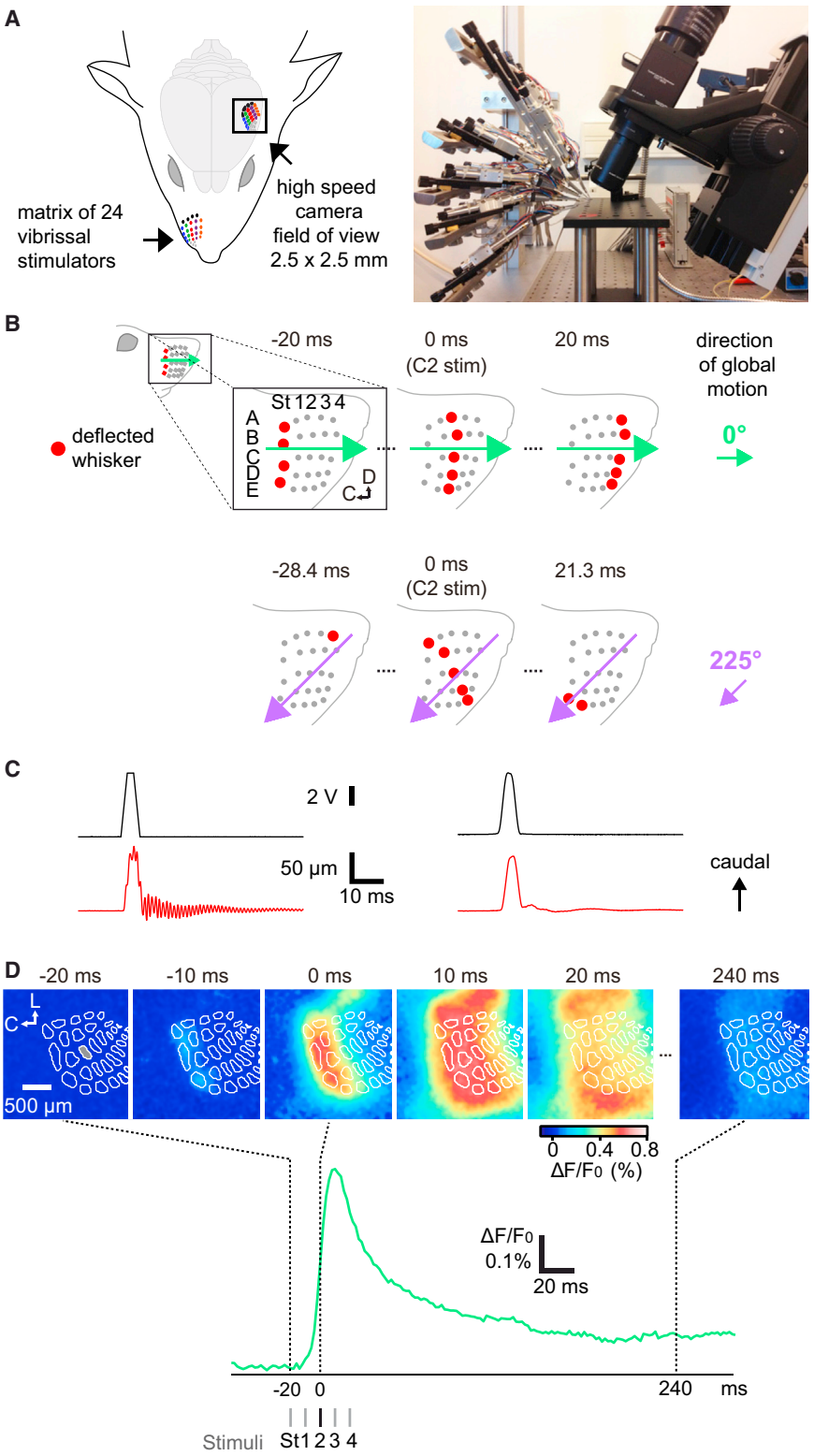

Figure 1. VSD Imaging of Cortical Responses to Multi-whisker Stimulation

(A) Scheme and photograph of the experimental setup. The left barrel cortex is imaged using a high-speed imaging system while the whiskers on the right side of the snout are stimulated with a 24-whisker stimulator.

(B) Global motion protocol. On the whisker pad, rows are named with letters and arcs with numbers, except the more caudal arc that corresponds to the four straddlers (St). Caudal (C) is left; dorsal (D) is up. These conventions apply to all figures. Three steps corresponding to two directions of the global motion protocol (0° and 225°) are illustrated. Red dots indicate the whiskers that are deflected at the time indicated on top.

(C) Voltage command (black trace) sent to a whisker stimulator and the resulting deflection measured with a laser telemeter at the tip of a stimulator (red trace), before (left) and after (right) correction of the command to prevent mechanical ringing.

(D) Snapshots of the averaged fluorescence signal (n = 30 trials) for a representative case at six different timings relative to the time of deflection of the central C2 whisker for the rostral global direction (0°). The barrel map reconstructed from a post hoc cytochrome oxidase staining and overlaid onto the VSD signals is shown as white outlines. The profile of fluorescence measured from the C2 barrel-related column (the ROI of the column C2 is shown as a gray area on the −20 ms snapshot) is shown below. The dotted lines indicate the time of deflection of the first arc of whiskers (−20 ms), the central Arc 2 stimulation time (0 ms), and a later time, tens of milliseconds following the stimulation (+240 ms), corresponding to the last snapshot.

deflection of all whiskers from one arc or row (Figure S1). On average, the speed of the spread was 95.2 ± 19.3 µm/ms, about twice as fast as it would be if it were relying primarily on the sequential feedforward activation of the cortical columns, a value that could be estimated around ~27–38 µm/ms, from the interwhisker interval of the stimulus (10 ms) and the distance between cortical barrel-related columns (~270 µm inter-arc and 380 µm inter-row averaged distances from Knutsen et al., 2016). Comparing the 4 directions of global motion revealed a slightly lower velocity for dorsal (90°) compared to ventral (270°) global motions, which corroborates the longer latency of the response observed in the C2 column for the dorsal motion. The early spread velocity, however, did not differ significantly between the caudal and rostral directions.

Depending upon the direction of the global motion, cortical activation of the central C2 column differed both in amplitude and temporal dynamics (Figure 2C, bottom), suggesting that information about the global direction could be extracted at the level of a single column (C2 in this case).

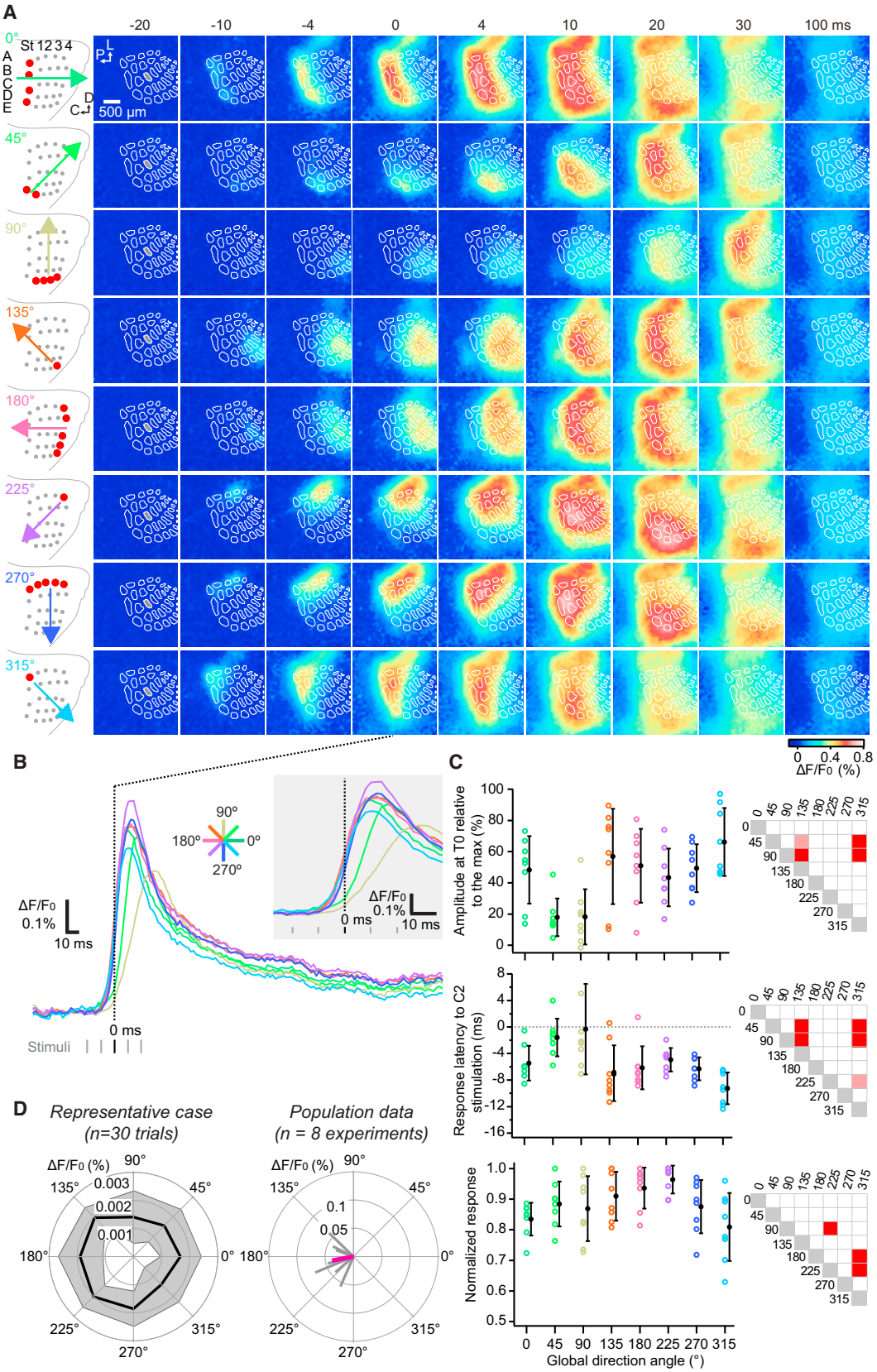

(legend on next page)

The C2 Barrel Column Shows Global Direction Selectivity Biased toward Caudo-ventral Directions

For the case illustrated in Figures 1, 2A, and 2B, the averaged responses were quantified over the C2 barrel-related column over a large time window (−20–240 ms) and represented on a polar plot (Figure 2D, left). The preferred direction was calculated (Experimental Procedures) and is shown as the thick vector whose length represents the vector summation. A bias toward caudo-ventral global direction can be observed in this case and in all the experiments (n = 8; Figure 2D, right) for the C2 barrel-related column (Rayleigh test; $p = 0.0015$).

These results suggest that neurons belonging to the C2 column in the mouse barrel cortex are tuned preferentially to caudo-ventral directions of global motions, consistent with observations in the rat barrel cortex (Jacob et al., 2008).

A Supra-barrel Distribution of Direction Selectivity to Global Motions Superimposed to the Somatotopic Map

To investigate the spatial organization of the direction selectivity to global motions for other barrel-related columns than C2, we computed the preferred direction and direction index for each column by aligning the profiles of VSD activity to the time of stimulation of its corresponding whisker (Experimental Procedures). The resulting direction selectivity and direction index maps for a representative case (same as illustrated in Figures 1 and 2) revealed that barrel-related columns corresponding to rostral whiskers show a significant anisotropic distribution of the direction selectivity with a bias toward caudo-ventral global motions (Rayleigh test; $p < 0.05$; dotted yellow outlines, Figure 3A). This distribution was more uniform in the columns corresponding to more caudal whiskers (Rayleigh test; $p > 0.05$). However, the direction selectivity for global motions is organized along a continuum, with the rostral columns presenting a direction preference with a strong caudal bias, the most lateral columns showing a caudo-ventral preference whereas the most caudal columns prefer ventral directions.

This spatial distribution of the direction preference for global motion was confirmed by analyzing 8 independent experiments (Figures 3B and 3C). For every barrel-related column, we computed a "similarity" value by comparing the preferred directions obtained for the eight experiments (Experimental Procedures). The similarity map confirmed a stronger directional preference for the more rostral columns. Direction selectivity was significant for the columns corresponding to the rostral whiskers (arcs 2–4; Rayleigh test; $p < 0.05$) and also for the alpha-whisker-related column (StA), which showed a significant selectivity toward the ventral direction (Rayleigh test; $p = 0.026$). Although the distribution of the direction index calculated for each experiment and each column reveals relatively small values, it is not centered at zero, which would be the case in the absence of direction selectivity for global motions.

The angular distribution of preferred directions for the eight individual experiments highlights the gradual spatial organization of direction selectivity to global motions across the barrel cortex (Figure 3C). It indeed illustrates the ventral bias for the caudal barrel-related columns, which is significant for the column corresponding to the dorsal alpha whisker (StA), but not for the columns corresponding to more ventral whiskers, such as gamma (StC). The angular distribution of preferred directions for global motions gradually becomes more anisotropic for the columns corresponding to rostral whiskers (as for C2 and C4 barrel-related columns in Figure 3C). The resulting directional bias gradually becomes strongly caudal for the most rostral columns (see the C4-related column in Figure 3C).

Additional VSD experiments were performed to test whether the selectivity to global motion depends on the direction of individual whisker deflections. Previous work suggested that it is not the case in the rat barrel cortex (Jacob et al., 2008). Whiskers were individually deflected in one of the 4 cardinal directions (caudal, ventral, rostral, or dorsal) within spatiotemporal sequences generating global motions in 8 different directions (n = 6 mice). Our results (Figures S2 and S3) show that congruent stimuli (similar direction of individual whisker deflections and global motion) do not systematically induce higher evoked responses when compared to non-congruent stimuli and that direction selectivity for global motions is not biased toward the direction of the individual whisker deflection.

The impact of the apparent speed of the global motions on the global direction selectivity was also tested in three additional experiments (Figure S4). Global motions were presented either like in the original protocol with an inter-whisker interval (IWI) of 10 ms or with a shortened IWI of 1 ms. In this second configuration, feedforward activity is likely to activate the consecutive columns faster than the cortico-cortical spread of activity. The spatial

Figure 2. Local Cortical Activation Depends on the Spatio-temporal Sequence of Multi-whisker Deflections

(A) Snapshots of the averaged fluorescence signals (same case as in Figure 1C) for the eight global directions (shown on the left) at different timings relative to the central C2 whisker deflection (0 ms). The barrel map is shown as white outlines.

(B) Fluorescent profiles measured from the C2 barrel-related column (gray area indicated on the −20 ms snapshots) for the eight directions of global motion. Global directions are color coded. The dotted line indicates the time of whisker C2 deflection. The inset shows the initial activation with an expanded timescale.

(C) (Top) Percentage of the response at the time of C2 whisker deflection. (Middle) Latencies were quantified by calculating a linear regression from 20% to 80% of the peak of the response for each global direction. Latency 0 ms corresponds to the time of C2 whisker deflection. (Bottom) The integral of each profile was calculated within a time window of −20–240 ms and normalized, for each individual experiment, to the higher response. Open circles represent the individual experiments, and filled black circles represent the averages (n = 8 experiments). Error bars correspond to the SD. Statistical tests are shown on the right: Friedman repeated-measures ANOVA on ranks followed by a Tukey test for multiple comparisons for the upper two and one-way ANOVA for repeated measures followed by the Holm-Sidak method for the lower one. Pale red, $p < 0.05$; red, $p < 0.01$.

(D) (Left) Polar plot of the averaged responses quantified over the C2 column for the representative case, integrated along a time window of −20–240 ms. The thick vector shows the preferred angle (color coded), and the length of the vector shows the vector sum of the responses (direction index: 0.074). The gray shadow corresponds to the SD (n = 30 repetitions). (Right) The distribution of global direction vectors for eight experiments (gray vectors) and the average (colored vector), calculated for the C2 column, are shown.

See also Figure S1.

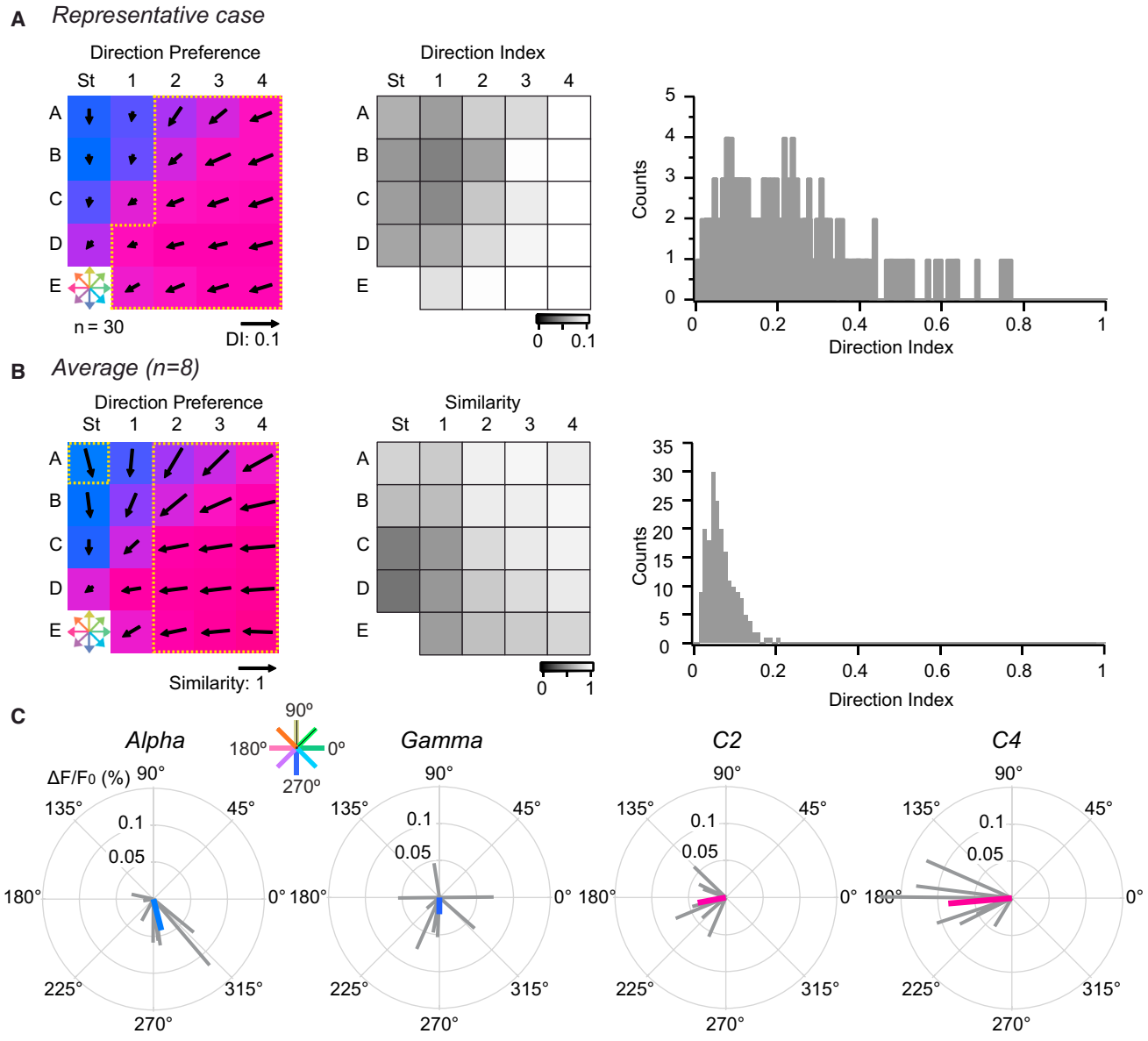

Figure 3. Spatial Distribution of Direction Selectivity to Global Motion

(A) 24-whisker map of direction preferences obtained for a representative case (left). For each barrel, the direction preference is color coded and represented by the angle of the arrow; the length of the arrow represents the direction index. The anisotropy of the direction preference distribution was evaluated with a Rayleigh test (over the 30 repetitions), and its significance ($p < 0.05$) is indicated by the dotted yellow contour. In the middle is represented a 24-whisker map of direction indexes. The histogram on the right shows the direction index values calculated individually for the 30 repetitions of the protocol and for the 24 barrel-related columns (n = 720 values; bin size: 0.01).

(B) Averaged 24-whisker map of direction preferences (n = 8 mice, left). The direction preference is color coded and represented by the angle of the arrows; the length of the arrow represents the similarity index between experiments and the significant anisotropic barrels (Rayleigh test; $p < 0.05$) are indicated by dotted yellow contours. In the middle is represented a 24-whisker map of similarity indexes. The histogram on the right shows the distribution of the direction indexes computed for all experiments and each barrel column (n = 192 values; bin size: 0.01).

(C) Representative angular distributions of preferred directions for global motion for each experiment (gray vectors) shown for the barrel columns that correspond to the whiskers alpha (StA), gamma (StC), C2, and C4. Vector sums for the 8 experiments, shown as colored vectors, indicate the averaged direction preferences. See also Figures S2, S3, and S4.

organization of direction selectivity for global motion was not affected with short IWI, although we observed a decrease in selectivity in this condition. Thus, as in the rat barrel cortex (Jacob et al., 2008), global direction selectivity can be revealed for a range of interstimulus intervals, but there is a limited dependence of the tuning strength on the apparent speed of the stimulus.

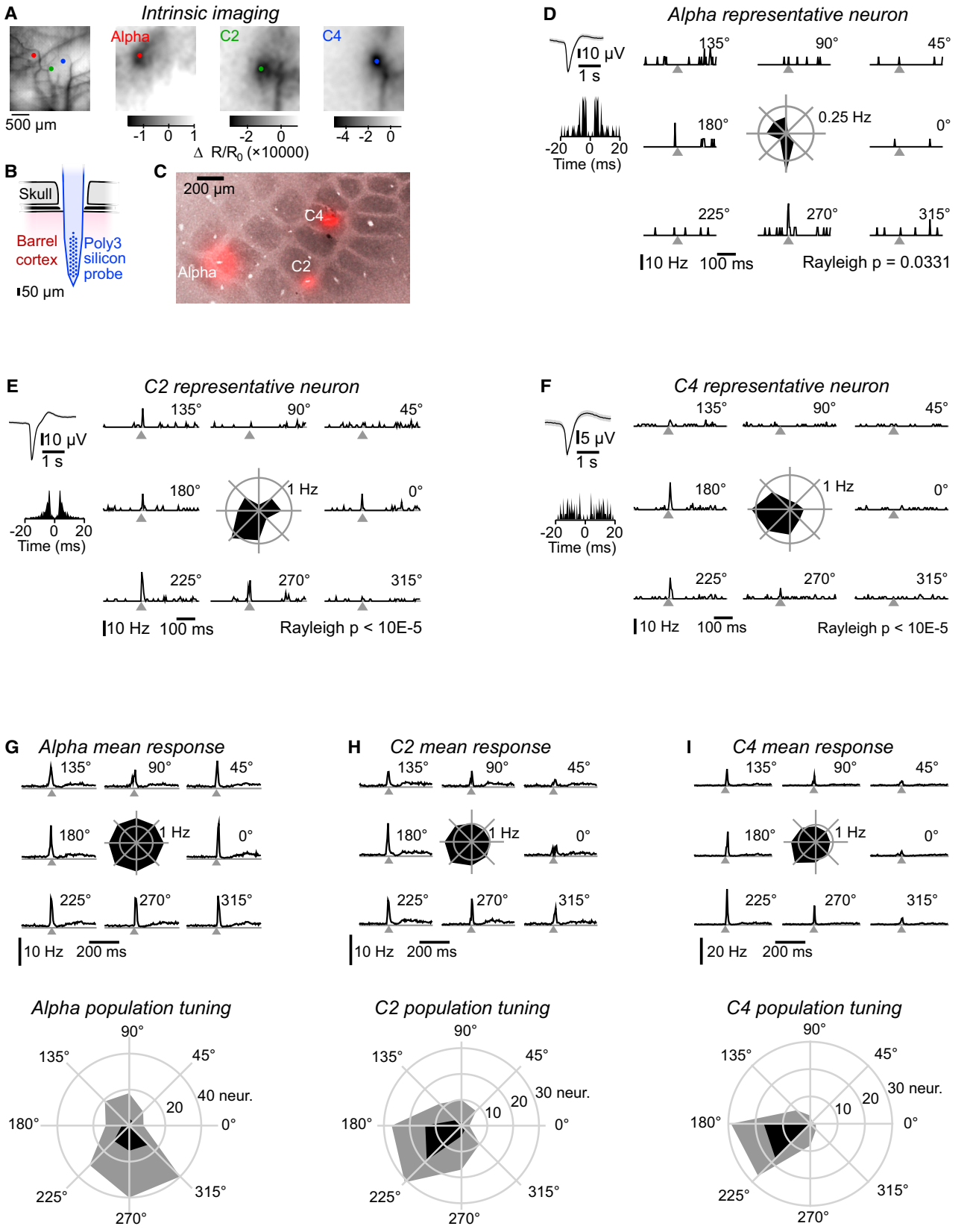

(legend on next page)

Electrophysiological Recordings Confirm the Spatial Organization of Direction Selectivity to Global Motions

To firm up the observation of a supra-barrel gradient of directional tuning, we performed extracellular recordings in 5 additional mice (Supplemental Experimental Procedures). We first used intrinsic imaging to functionally locate three barrels, corresponding to the straddler alpha (StA), the C2, and the C4 whiskers (Figure 4A). At these locations, we performed a craniotomy and inserted a Poly3 silicon probe into the cortex at depths ranging from 200 to 600 μm below the cortical surface (Figure 4B). We recorded extracellular spiking activity in the barrels while applying the same multi-whisker stimulation protocol that was performed during VSD experiments. After recordings were done, cytochrome oxidase staining of tangential sections of the barrel cortex combined with DiI marks left by the electrode validated the positioning of the electrode with respect to layer 4 barrels (Figure 4C).

For each target whisker (StA, C2, and C4), we grouped units that were recorded at most ½ barrel away from the target barrel, according to the histology. Consistent with the VSD-based findings, units near StA were often tuned to ventral global motion (case study in Figure 4D), whereas C2 units preferred ventro-rostral motion (Figure 4E), and for C4 units, caudal motion was predominant (Figure 4F). These findings were confirmed at a population level by looking both at population average firing rate and the distribution of the preferred global motion direction of the neurons (Figures 4G–4I). Overall, in the three points of the barrel map that we have explored, the distribution of the neurons' tuning was consistent with the VSD results described in Figure 3, both for neurons with a significant direction preference (Rayleigh $p < 0.05$) and when looking at the direction preference of all recorded neurons (Figures 4G–4I).

Cortical Responses to Global Motions Are Highly Sublinear

To further understand the mechanisms for global direction selectivity and its distribution over the barrel field of the somatosensory cortex, we first hypothesized that the direction selectivity to global motions might be determined by the suppressive interactions that have been reported when adjacent whiskers are sequentially deflected (Brumberg et al., 1996; Civillico and Contreras, 2006; Ego-Stengel et al., 2005; Higley and Contreras, 2005; Jacob et al., 2008; Kleinfeld and Delaney, 1996; Simons, 1985; Simons and Carvell, 1989). To test this hypothesis, we designed a protocol in which we randomly alternated two types of stimulations: global motions in four cardinal directions (moving bars, Figure 5A) and the stimulation of individual rows or arcs (static bars, Figure 5B). By linearly adding up the responses to the static bars, we constructed linear predictions of the responses to the moving bars (Figure 5C). A representative example of the rostral global motion (0°) is illustrated in Figure 5, with snapshots of the activity over the barrel cortex at the time of stimulation of the indicated whiskers.

By comparing the evoked responses to global motions (moving bars, blue lines) with the corresponding linear predictions (green lines), we observed that the linear summations reached much higher levels of activation (Figure 6A). This indicates that suppressive mechanisms are involved in shaping the cortical responses to global motions. We next quantified these sublinearities and tested whether they depend upon the direction of the global stimulation. For five independent experiments, we calculated the integral of responses (moving bars and linear summations) from a ROI corresponding to the C2 barrel-related column (Figure 6B) within a time window of −20–240 ms and for the four cardinal directions. The ratio of moving bar responses over linearly predicted responses is overall 0.30 ± 0.03 ($n = 5$ experiments). This ratio does not differ according to the direction of stimulation (one-way ANOVA for repeated measures; $p = 0.1$).

To assess whether the sublinearities could nevertheless be determinant to encode the direction of the global motion, we computed the direction selectivity map that would result from the linear predictions of the responses to moving bars. The direction selectivity map obtained from the linear predictions ($n = 5$ experiments) is qualitatively different from the one obtained from the responses to moving bars (Figure 6C). Only some columns—located mainly on the borders of the barrel field—showed a significant preferred direction (Rayleigh test; $p < 0.05$; dotted yellow outlines), with angles distributed in an inversed pinwheel, pointing toward the borders of the field. This inversed pinwheel is expected given that the linear prediction responses are obtained by sequentially adding the responses to the static bars. The border columns are expected

Figure 4. Extracellular Recordings Confirm the Spatial Organization of Direction Selectivity

(A) (Left) Blood vessel pattern at barrel cortex surface visualized through the intact skull under green illumination. (Right) Intrinsic optical signals imaged through the bone in response to the stimulation (100 Hz; 1 s) of whiskers alpha, C2, and C4 are shown.

(B) Insertion of Poly3 silicon probe in a localized craniotomy.

(C) DiI mark left by probe insertion in the three recording sites, shown in a tangential slice of the barrel cortex. Barrels are highlighted using post hoc cytochrome oxidase staining.

(D) Global motion direction tuning of a representative unit recorded in the alpha barrel. (Left margin, top) Largest spike shape recorded across the channels is shown (Light background: SEM). (Left margin, bottom) Autocorrelogram. (Right) Peristimulus time histogram (PSTH) for the 8 directions of global motion stimuli, and at the center, a polar plot of the mean firing rate in a window (−20–240 ms) aligned on alpha whisker stimulations (gray arrowhead) across the 8 bar directions is shown.

(E) Same as (D) for a C2 representative unit.

(F) Same as (D) for a C4 representative unit.

(G) (Top) Averaged PSTHs and polar plot of the mean firing rate around stimulus for the 58 units with a significant tuning to the global motion stimulus direction (Rayleigh $p < 0.05$), recorded close to the alpha barrel in 3 mice. (Bottom) Population histogram of the preferred global direction for significantly tuned units (black) and for all units recorded close to the alpha barrel (187 units, gray).

(H) Same as (G) for 45 significantly direction-tuned units recorded in 5 mice and for a total of 126 units recorded close to the C2 barrel.

(I) Same as (G) for 35 significantly direction-tuned units recorded in 2 mice and for a total of 81 units recorded close to the C4 barrel.

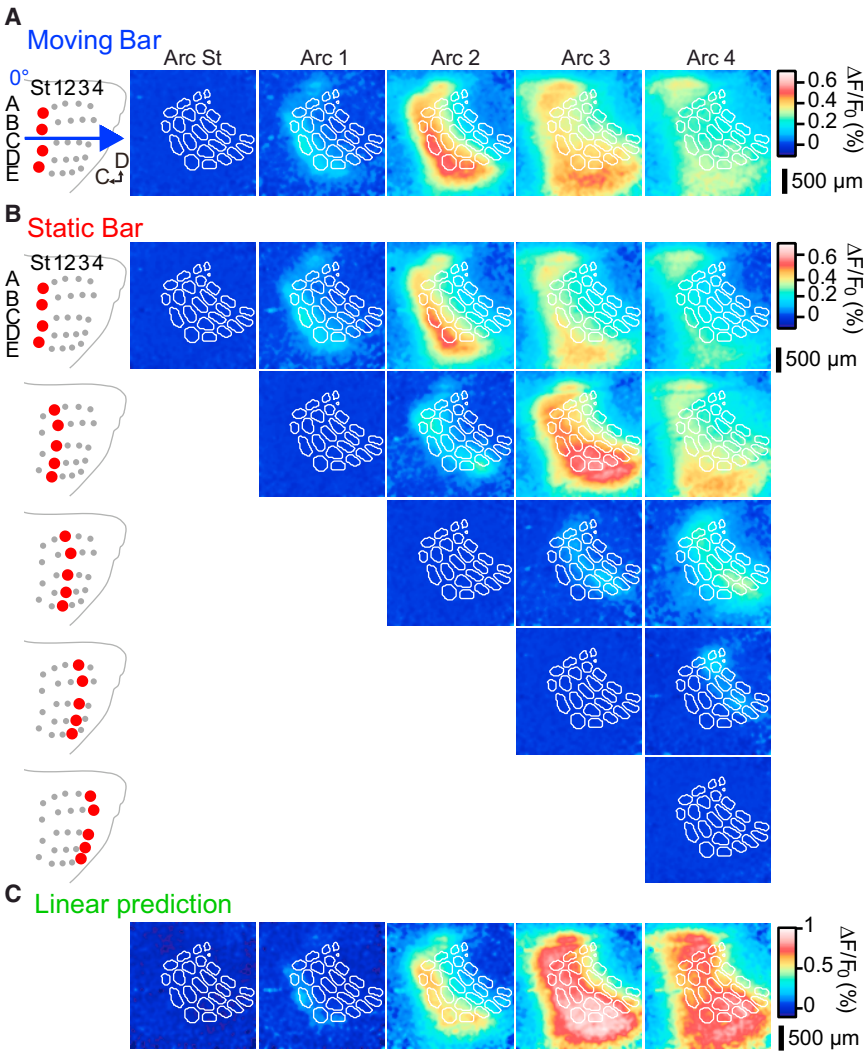

Figure 5. Moving/Static Bar Protocols and Linear Prediction

(A) Illustration of the moving bar stimulus for 0° direction with snapshots of the cortical response observed for a representative case, at the time of deflection of each arc (n = 30 repetitions).

(B) Examples of static bar stimuli. Snapshots of cortical activity evoked by the stimulation of the arc indicated on the left (averaged over 30 repetitions) are shown for the same case as in (A) at the time of deflection of each arc and subsequently every 10 ms.

(C) Linear prediction of cortical activity evoked by a moving bar stimulus for 0° direction computed as the sum of the responses to static bar stimuli at times that match the moving bar. Snapshots of the summed cortical activity (n = 30 repetitions) for the same case as in (A) and (B) are shown, computed at the time of deflection of each arc.

to show a larger response for the direction that activates first the columns of the opposite side of the barrel field. The distribution of the corresponding direction index for all the columns (n = 24) and all the experiments (n = 5; Figure 6C, bottom left) shows most values close to zero in the case of the linear prediction model, confirming that the majority of the columns do not present significant direction selectivity under the linear assumption.

To quantify the differences between the two maps, we computed for each barrel-related column the angular difference between the direction preference obtained from the linear prediction and the one obtained from responses to the moving bars (Figure 6D). This angular difference (in average of 127° ± 59°) was large for most of the columns, especially in the barrel columns corresponding to the more rostral and dorsal whiskers, which are the ones that show significant direction selectivity with the moving bar protocol.

These results therefore indicate that the observed spatial organization of direction selectivity for global motions emerges from sublinear interactions.

Direction Selectivity to Global Motion Does Not Only Rely on the Identity of the First Stimulated Whiskers

Images of the early cortical activation evoked by a moving bar look very similar to the ones obtained in response to a static bar, where only the first row or arc at the border of the barrel field (arc St, arc 4, row A, or row E) is stimulated (henceforth "front static bar"). To quantitatively compare these cortical responses, we integrated them along a time window of −20–240 ms and over a ROI corresponding to the C2 column (Figure 7A). We found that responses for the front static and moving bars did not differ significantly (one-way ANOVA for repeated measures; p = 0.077). The ratio of the responses to the front static bar over the moving bar was overall 0.58 ± 0.12 and did not differ significantly according to the direction (Figure 7B; n = 5 experiments).

To further assess whether the spatial distribution of selectivity to the direction of global motion could result from the salience of the starting position of the moving bar, we computed a direction selectivity map using the responses to the front static bars: arc St; arc 4; row A; and row E (n = 5 experiments). This map shows a pinwheel-like distribution of the preferred directions, with the center close to the column D3 (Figure 7C, left). Both the direction selectivity maps and the direction index distributions differed between front static bar and moving bar conditions (Figure 7C, right). By computing the angular difference between the two direction selectivity maps, we observed that only few columns among the ones corresponding to the most dorsal and rostral whiskers share comparable direction preference in both conditions (Figure 7D). The preferred directions differed on average from 83° ± 46° between the two conditions.

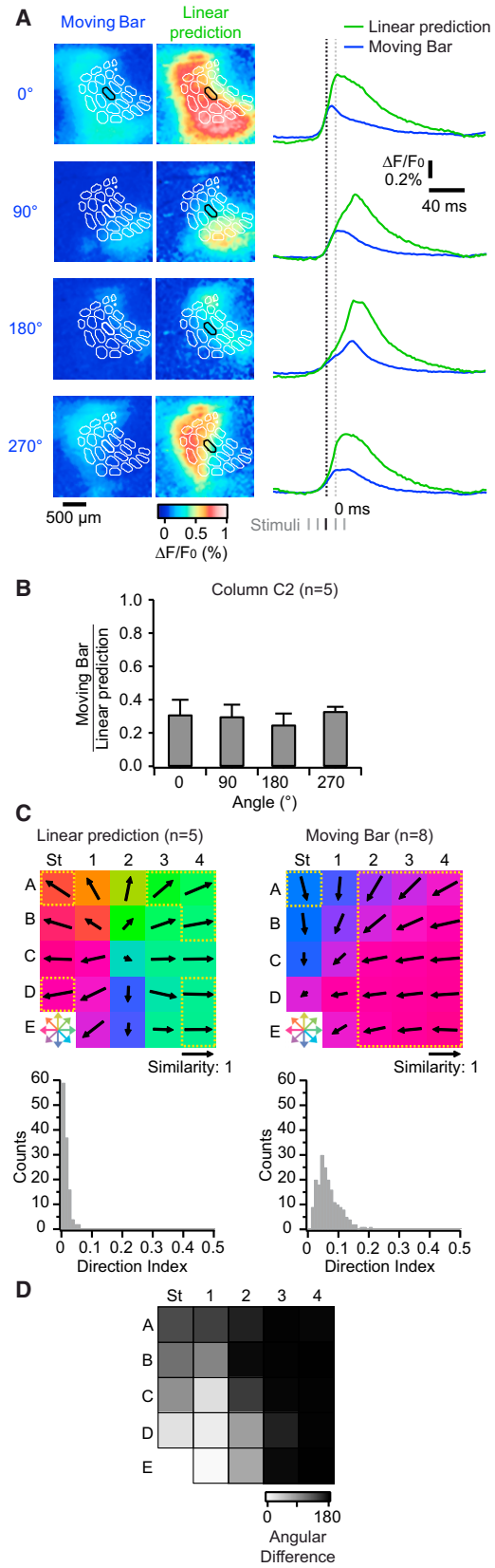

Figure 6. Cortical Responses to a Moving Bar Are Highly Sublinear

(A) Comparison of the cortical activity evoked by moving bars and their corresponding linear prediction. (Left) Snapshots of the responses at 30 ms following the beginning of the stimulation for four global directions (0°, 90°, 180°, and 270°) of the moving bar (n = 30 trials) and their corresponding linear prediction from static bar responses summation (same fluorescence scale) are shown. (Right) Profiles of activity calculated from the C2 barrel-related column for the moving bar and linearly predicted responses are shown. The vertical bars below indicate the time of stimulation of arcs/rows, the time of deflection of the Arc 2 being in black and indicated by the long black dotted line. The gray dotted line indicates the time +30 ms of the snapshots shown on the left.

(B) Population ratios (n = 5 experiments) of responses to the moving bar and the linear prediction computed from the C2 column over a time window of −20–240 ms for the different directions. Error bars correspond to the SD.

(C) (Left) Averaged 24-whisker map of direction preference (n = 5 experiments) for the linear prediction and histogram of the corresponding direction indexes (n = 120 values; bin size: 0.01). (Right) Moving bar map and histogram (as in Figure 3B) are shown.

(D) Angular difference map between the preferred angles of the linear prediction and the moving bar responses.

These results suggest that, although the salience of the starting position of the moving bar might participate in part to the emergence of the spatial distribution of the global direction selectivity, other mechanisms that build up when the bar is moving across the whisker pad are also required.

DISCUSSION

Emergence of Direction Selectivity to Global Motion

Is direction selectivity to global motion emerging in the cortex or in subcortical structures? Direction selectivity to global motion is already present at the level of the ventral posterior medial nucleus of the thalamus (VPM) in the rat (Ego-Stengel et al., 2012), but it is amplified in the cortex. Indeed, VPM selectivity decreased under cortical inactivation. Moreover, stimulating the closest adjacent whiskers or including the more distant ones from the principal whisker does not change selectivity in VPM, whereas it increases selectivity in the cortex.

In 2010, Wilson and collaborators proposed a computational model to explain the emergence of local direction selectivity maps in L2/3 of the rat barrel cortex (Wilson et al., 2010). This model generates predictions about the spatial organization of local direction selectivity (i.e., the preference for a given direction of deflection of the principal whisker), not only within single columns but also at the scale of the entire barrel field. The level of correlation between the individual whisker deflections and the global stimulus during the training of the network strongly influences the supra-columnar spatial distribution of local direction selectivity. It is therefore likely that the input statistics can also shape the supra-columnar organization of direction selectivity for global motion in an experience-dependent manner.

Both in barrel cortex and VPM, the responses recorded extracellularly to global motion protocols and to only one whisker deflection were similar (Ego-Stengel et al., 2012; Jacob et al., 2008). The nonlinearities involved in the generation of the global direction selectivity are therefore likely to be suppressive rather than facilitatory, such as the ones involved in cross-whisker suppressive interactions in VPM and cortex (Brumberg et al., 1996; Civillico and Contreras, 2006; Ego-Stengel et al., 2005; Higley

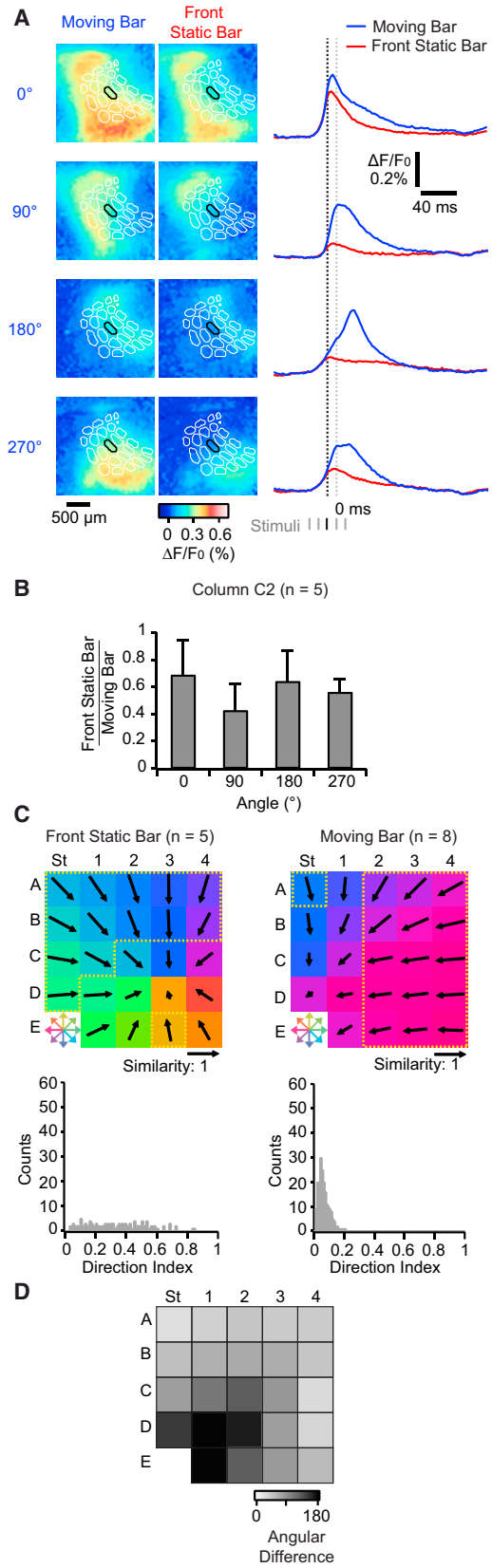

Figure 7. Global Direction Selectivity Does Not Only Rely on the Starting Position of the Moving Bar

(A) Comparison of the cortical activity evoked by moving bars and their corresponding front static bars where only the first row or arc of whiskers is stimulated. (Left) Snapshots of the responses at 30 ms following the beginning of the stimulation for four global directions (0°, 90°, 180°, and 270°) of the moving bar (n = 30 trials) and their corresponding front static bars (same fluorescence scale) are shown. (Right) Profiles of activity calculated from the C2 barrel-related column for moving bar and front static bar responses are shown. Same conventions as in Figure 5A for the vertical bars below and the dotted lines are shown.

(B) Population ratios (n = 5 experiments) of responses to the static bar and the moving bar computed from the C2 column over a time window of −20–240 ms for the different directions. Error bars correspond to the SD.

(C) (Left) Averaged 24-whisker map of direction preference (n = 5 experiments) for the front static bar and histogram of the corresponding direction indexes (n = 120 values; bin size: 0.01). (Right) Moving bar map and histogram are shown (as shown in Figure 3B).

(D) Angular difference map between the preferred angles of the front static bar and the moving bar responses.

and Contreras, 2003, 2005; Kleinfeld and Delaney, 1996; Shimegi et al., 1999, 2000; Simons, 1985; Simons and Carvell, 1989).

At the single-neuron level, linear summation of the responses to single-whisker deflections failed to explain the selectivity to global motion (Jacob et al., 2008). Here, we constructed a linear prediction of the response to global motion by sequentially adding the responses to the stimulation of individual arcs or rows. Linear summation of the responses to a group of whiskers (arcs or rows) also failed to explain the global direction selectivity. Cortical activation induced by such sequential stimuli is highly sublinear.

Importance of Cortical Nonlinearities

The starting point of a front edge crossing the whiskers has a strong impact on cortical responses (Drew and Feldman, 2007). Thus, the spatial distribution of the global direction selectivity could be influenced by the starting position of the moving bar. To test this hypothesis, we compared the direction selectivity maps obtained with the moving bar protocol and with the deflection of the first arcs or rows (front static bar protocol). The two maps differed significantly, with rostral and dorsal directions more represented using the front static bar protocol and a bias toward the caudal direction for the moving bar protocol. The direction preferences observed with the front static bar protocol are likely to result from functional asymmetries of the barrel cortex, with stronger responses to the deflection of the large caudal whiskers (straddlers) than to the small rostral whiskers (belonging to arc 4) and, similarly, larger responses to row A than row E.

The differences between the two maps suggest that the global direction selectivity emerges when sequentially deflecting all the whiskers. These results are in agreement with previous recordings of neuronal responses to proximal (stimulating only 9 whiskers) and global stimuli (24 whiskers), which revealed that all the whiskers need to be deflected to observe a significant global direction selectivity in the rat barrel cortex (Jacob et al., 2008). Drew and Feldman (2007) deflected only 9–12 whiskers, which might explain the lack of direction selectivity reported in their

study. This long range integration is originating in the cortex because applying the protocol to only 9 whiskers had little influence on the selectivity of VPM neurons (Ego-Stengel et al., 2012).

Selectivity to Natural Statistics of the Stimulus

Our results showed a caudo-ventral bias for preferred directions of global motions, consistent with our previous results (Jacob et al., 2008) for the C2 barrel-related column in the rat. This bias is also spatially distributed: rostral columns preferred caudal global directions whereas dorsal columns tend to prefer ventral global directions.

Why do caudal and ventral global directions of stimulation elicit the largest responses in the majority of the barrel-related columns? We recorded the profile of a running mouse and observed that the rows of whiskers are not horizontal but oriented about 40° downward (data not shown). With such head position, the global direction of deflection of the whiskers during classical thigmotactic behavior is in the caudo-ventral axis. A higher cortical representation of global caudo-ventral stimuli could reflect experience-dependent, adaptive mechanisms leading to higher sensitivity to the most frequent stimuli. Indeed, given that the rat intrabarrel direction selectivity maps emerge late in development and are likely to be shaped by experience-dependent plasticity (Kremer et al., 2011, Wilson et al., 2010), we can hypothesize that the same might happen to global direction selectivity maps. Further studies of the statistics of the mouse natural tactile inputs should be conducted to understand the emergence of direction selectivity to global motion.

To conclude, here, we showed that the mouse barrel cortex is able to extract the global direction of a multi-whisker moving stimulus. This form of direction selectivity emerges from nonlinear interactions and is spatially distributed over the topographic arrangement of barrels in a supra-barrel manner. How this distribution is exploited by the cerebral cortex to construct a global percept of a moving object is still unknown. A supra-barrel organization could be computationally advantageous in conveying stimulus information into higher brain areas (Thivierge and Marcus, 2007). It could be used to discriminate stimulus features, such as orientation of object movements (Polley et al., 2005) or self-movement. Higher order areas, such as the secondary somatosensory cortex, which likely integrates tactile sensory information over larger time and spatial scales, might play a role in the functional readout. Future studies focusing on the integration of multi-whisker inputs within this cortical area are needed to further understand the cortical processing of complex tactile scenes.

EXPERIMENTAL PROCEDURES

Animals and Surgery

Experiments were performed in conformity with French and European (2010/63/UE) legislations on animal experimentation (authorization number: 2012-0068 delivered by the local ethical committee no. 59). VSD imaging was performed on male or female 6- to 10-week-old C57BL6J mice under urethane (1.7 mg/g) or isoflurane (induction 3%–4%; maintenance 1%–1.5%) anesthesia. Paw withdrawal, whisker movement, and eye-blink reflexes were suppressed by the anesthesia. Body temperature was maintained at 37°C. Respiration was monitored with a piezoelectric device. Brain state was monitored by using epidural electrodes above the barrel cortex and the frontal cortex ipsilateral to the stimulated whiskers. A metallic post was solidly glued on the occipital bone. A 3 × 3 mm craniotomy centered on the stereotaxic location of the C2 barrel column (1.5 mm caudal and 3.3 mm lateral) was made to expose the barrel cortex. Care was taken not to damage the cortex during the removal of the dura.

Voltage-Sensitive Dye Imaging

The voltage-sensitive dye RH1691 (Optical Imaging, Israel) was dissolved at 1 mg/mL in Ringer's solution containing (in mM) 135 NaCl, 5 KCl, 5 HEPES, 1.8 CaCl2, and 1 MgCl2. It was topically applied to the exposed cortex and allowed to diffuse 1 hr into the cortex. After removal of the unbound dye, the cortex was covered with agarose (0.5%–1% in Ringer's) and a coverslip. Cortical imaging was performed through a tandem-lens fluorescence microscope (SciMedia, USA) equipped with one Leica PlanApo 5× (objective side) and one Leica PlanApo 1× (condensing side), a 100-W halogen lamp gated with an electronic shutter, a 630-nm excitation filter, a 650-nm dichroic mirror, and a long-pass 665-nm emission filter. Images were acquired with a high-speed MiCam Ultima camera (SciMedia, USA) at 500 Hz with a field of view of 2.5 × 2.5 mm, resulting in a pixel resolution of 25 × 25 μm. The illumination of the cortical surface started 500 ms before each image acquisition to avoid acquiring signal in the steeper phase of the fluorescence bleaching. Recordings were of 1 s duration with 200 ms baseline and 800 ms post-stimulation. Variations of the light intensity were initially recorded as variations over the resting light intensity (first acquired frame).

VSD Imaging Analysis

Acquisition and data preprocessing were done using in-house software (Elphy, G. Sadoc, UNIC-CNRS). Further analyses were with IgorPro (WaveMetrics, USA). For each experiment, all the blank trials were averaged together and subtracted pixel by pixel from each trial to correct for bleaching-related artifact.

Variations of the fluorescence signal are expressed as ΔF/F0, the averaged signal over three frames just preceding the stimulus being used as a reference (F0).

Profiles of fluorescence were computed from ROIs corresponding to the layer 4 barrels delineated from the post hoc barrel map reconstruction. Variations of fluorescence from all the pixels included in a barrel were averaged.

Whisker Stimulation

Deflections of the right 24 posterior macrovibrissae of the mice were performed using a multi-whisker stimulator (Jacob et al., 2010). The experimental imaging setup is shown in Figure 1A. Whiskers on the right side were cut to a length of 10 mm and inserted, keeping their natural angle in 27G stainless steel tubes attached to the piezoelectric benders (Noliac, Denmark), leaving 2 mm between the tip of the tube and the whisker base. Each whisker deflection consisted of a 95-μm displacement (measured at the tip of the tube), a 2-ms rising time, a 2-ms plateau, and a 2-ms fall. The deflection amplitude of each actuator was calibrated using a laser telemeter (Micro-Epsilon, France), and specific filters were applied to the voltage commands to prevent mechanical ringing of the stimulators (Figure 1C). The resulting initial deflection velocity was of 1,270°/s.

Multi-whisker Global Motion Protocol

The 24 whiskers were stimulated either in the caudal or rostral direction within spatiotemporal sequences generating global motions in eight different directions (Jacob et al., 2008). The sweep duration in the horizontal and vertical axes was 46 ms (interval between two consecutive stimulated arcs or rows or IWI: 10 ms); the whisker C2 was deflected 20 ms after the beginning of the sweep. For oblique directions, a sweep lasted 62.57 ms (IWI: $10/\sqrt{2}$ = 7.1 ms), and the whisker C2 was stimulated 28.3 ms after the beginning of the protocol.

During VSD imaging experiments, the eight global motion stimuli together with an extra blank trial (no stimulation) were presented 30 times in a pseudo-randomized way. Two consecutive sequences were separated by a 15-s interval. For electrophysiological recordings, the interval between two consecutive global motion stimuli was shortened to 2 s. Continuous

recordings were made during about 1 hr, resulting in more than 1,500 trials per direction of global motion.

Multi-whisker Moving/Static Bar Protocols

All the whiskers were deflected as described above, in the caudal direction (Figure 1C). For the moving bar condition, the 24 macrovibrissae were stimulated with spatiotemporal sequences generating global motions as described above but only in the four cardinal directions (IWI: 10 ms). The static bar sequences consisted of deflecting the 5 arcs and the 5 rows of whiskers independently of each other. In total, four moving bar and ten static bar stimuli, together with two blank trials, were repeated 30 times in a pseudo-randomized way. An interval of 15 s was applied between two consecutive sequences.

Direction Selectivity

The response magnitude (Ri) to each direction (θi) of stimulation was defined as the integral of the fluorescence profiles (for VSD imaging) or mean firing rate (for extracellular recordings) on a large time window (−20–240 ms relative to the time of stimulation of the corresponding whisker). The preferred direction (Dpref) was defined as the circular mean (Fisher, 1995):

$$Dpref = \arctan\left[\sum Risin(\theta i) \Big/ \sum Ricos(\theta i)\right].$$

To quantify the Dpref, the direction index (DI) was defined as

$$DI = \sqrt{\left[\sum Risin(\theta i)\right]^2 + \left[\sum Ricos(\theta i)\right]^2} \Big/ \sum Ri.$$

The DI takes values from 0 (equal responses to all directions) to 1 (complete selectivity to one direction).

Likewise, we quantified the similarity between the Dprefs for barrel across the different experiments, defining the similarity index (SI) as

$$SI = \sqrt{\left[\sum Disin(Dpref)\right]^2 + \left[\sum Dicos(Dpref)\right]^2} \Big/ \sum Di.$$

The SI takes values from 0 (different Dpref between experiments) to 1 (equal Dpref).

Statistical Tests

Rayleigh test of circular uniformity was used to test the significance of the direction selectivity, analyzing the distribution of the preferred direction angles for the different experiments in each barrel.

Other quantifications were analyzed using the SigmaStat software (Systat, USA) by one-way ANOVA for repeated measures followed by the Holm-Sidak method for multiple comparisons or, if the normality test failed, by Friedman repeated-measures ANOVA on ranks followed by a Tukey test for multiple comparisons.

SUPPLEMENTAL INFORMATION

Supplemental Information includes Supplemental Experimental Procedures and four figures and can be found with this article online at https://doi.org/10.1016/j.celrep.2018.03.006.

ACKNOWLEDGMENTS

This work was supported by the Centre National de la Recherche Scientifique (France), the European Union Seventh Framework Programme BrainScaleS (FP7-ICT-2009-6 and N 269921), the Agence Nationale pour la Recherche (SensoryProcessing, Transtact), the Region Ile de France (DIM Nano-K, ML02 Neurofib), and the Lidex Neuro-Saclay. We thank Gérard Sadoc, Guillaume Hucher, and Aurélie Daret for technical and experimental assistance.

AUTHOR CONTRIBUTIONS

Conceptualization, D.E.S. and I.F.; Methodology, M.E.V., L.E., D.E.S., and I.F.; Software, M.E.V., L.E., and I.F.; Investigation, M.E.V., L.E., and I.F.; Formal Analysis, M.E.V., L.E., and I.F.; Writing – Original Draft, M.E.V.; Writing – Review & Editing, L.E., D.E.S., and I.F.; Funding Acquisition, D.E.S. and I.F.; Supervision, D.E.S. and I.F.

DECLARATION OF INTERESTS

The authors declare no competing interests.

Received: March 21, 2017
Revised: January 17, 2018
Accepted: February 28, 2018
Published: March 27, 2018

REFERENCES

Andermann, M.L., and Moore, C.I. (2006). A somatotopic map of vibrissa motion direction within a barrel column. Nat. Neurosci. *9*, 543–551.

Armstrong-James, M., and Callahan, C.A. (1991). Thalamo-cortical processing of vibrissal information in the rat. II. spatiotemporal convergence in the thalamic ventroposterior medial nucleus (VPm) and its relevance to generation of receptive fields of S1 cortical "barrel" neurones. J. Comp. Neurol. *303*, 211–224.

Arnold, P.B., Li, C.X., and Waters, R.S. (2001). Thalamocortical arbors extend beyond single cortical barrels: an in vivo intracellular tracing study in rat. Exp. Brain Res. *136*, 152–168.

Brecht, M., and Sakmann, B. (2002). Dynamic representation of whisker deflection by synaptic potentials in spiny stellate and pyramidal cells in the barrels and septa of layer 4 rat somatosensory cortex. J. Physiol. *543*, 49–70.

Brecht, M., Roth, A., and Sakmann, B. (2003). Dynamic receptive fields of reconstructed pyramidal cells in layers 3 and 2 of rat somatosensory barrel cortex. J. Physiol. *553*, 243–265.

Brumberg, J.C., Pinto, D.J., and Simons, D.J. (1996). Spatial gradients and inhibitory summation in the rat whisker barrel system. J. Neurophysiol. *76*, 130–140.

Carvell, G.E., and Simons, D.J. (1986). Somatotopic organization of the second somatosensory area (SII) in the cerebral cortex of the mouse. Somatosens. Res. *3*, 213–237.

Civillico, E.F., and Contreras, D. (2006). Integration of evoked responses in supragranular cortex studied with optical recordings in vivo. J. Neurophysiol. *96*, 336–351.

Drew, P.J., and Feldman, D.E. (2007). Representation of moving wavefronts of whisker deflection in rat somatosensory cortex. J. Neurophysiol. *98*, 1566–1580.

Ego-Stengel, V., Mello e Souza, T., Jacob, V., and Shulz, D.E. (2005). Spatiotemporal characteristics of neuronal sensory integration in the barrel cortex of the rat. J. Neurophysiol. *93*, 1450–1467.

Ego-Stengel, V., Le Cam, J., and Shulz, D.E. (2012). Coding of apparent motion in the thalamic nucleus of the rat vibrissal somatosensory system. J. Neurosci. *32*, 3339–3351.

Feldmeyer, D., Brecht, M., Helmchen, F., Petersen, C.C.H., Poulet, J.F.A., Staiger, J.F., Luhmann, H.J., and Schwarz, C. (2013). Barrel cortex function. Prog. Neurobiol. *103*, 3–27.

Fisher, N.I. (1995). Statistical Analysis of Circular Data (Cambridge University Press).

Higley, M.J., and Contreras, D. (2003). Nonlinear integration of sensory responses in the rat barrel cortex: an intracellular study in vivo. J. Neurosci. *23*, 10190–10200.

Higley, M.J., and Contreras, D. (2005). Integration of synaptic responses to neighboring whiskers in rat barrel cortex in vivo. J. Neurophysiol. *93*, 1920–1934.

Hubel, D.H., and Wiesel, T.N. (1963). Shape and arrangement of columns in cat's striate cortex. J. Physiol. *165*, 559–568.

Hübener, M., Shoham, D., Grinvald, A., and Bonhoeffer, T. (1997). Spatial relationships among three columnar systems in cat area 17. J. Neurosci. *17*, 9270–9284.

Jacob, V., Le Cam, J., Ego-Stengel, V., and Shulz, D.E. (2008). Emergent properties of tactile scenes selectively activate barrel cortex neurons. Neuron *60*, 1112–1125.

Jacob, V., Estebanez, L., Le Cam, J., Tiercelin, J.-Y., Parra, P., Parésys, G., and Shulz, D.E. (2010). The Matrix: a new tool for probing the whisker-to-barrel system with natural stimuli. J. Neurosci. Methods *189*, 65–74.

Kim, U., and Ebner, F.F. (1999). Barrels and septa: separate circuits in rat barrels field cortex. J. Comp. Neurol. *408*, 489–505.

Kleinfeld, D., and Delaney, K.R. (1996). Distributed representation of vibrissa movement in the upper layers of somatosensory cortex revealed with voltage-sensitive dyes. J. Comp. Neurol. *375*, 89–108.

Knutsen, P.M., Mateo, C., and Kleinfeld, D. (2016). Precision mapping of the vibrissa representation within murine primary somatosensory cortex. Philos. Trans. R. Soc. Lond. B Biol. Sci. *371*, 20150351.

Kremer, Y., Léger, J.-F., Goodman, D., Brette, R., and Bourdieu, L. (2011). Late emergence of the vibrissa direction selectivity map in the rat barrel cortex. J. Neurosci. *31*, 10689–10700.

Le Cam, J., Estebanez, L., Jacob, V., and Shulz, D.E. (2011). Spatial structure of multiwhisker receptive fields in the barrel cortex is stimulus dependent. J. Neurophysiol. *106*, 986–998.

Manns, I.D., Sakmann, B., and Brecht, M. (2004). Sub- and suprathreshold receptive field properties of pyramidal neurones in layers 5A and 5B of rat somatosensory barrel cortex. J. Physiol. *556*, 601–622.

Moore, C.I., and Nelson, S.B. (1998). Spatio-temporal subthreshold receptive fields in the vibrissa representation of rat primary somatosensory cortex. J. Neurophysiol. *80*, 2882–2892.

Narayanan, R.T., Egger, R., Johnson, A.S., Mansvelder, H.D., Sakmann, B., de Kock, C.P.J., and Oberlaender, M. (2015). Beyond Columnar Organization: Cell Type- and Target Layer-Specific Principles of Horizontal Axon Projection Patterns in Rat Vibrissal Cortex. Cereb. Cortex *25*, 4450–4468.

Perronnet, L., Vilarchao, M.E., Hucher, G., Shulz, D.E., Peyré, G., and Ferezou, I. (2016). An automated workflow for the anatomo-functional mapping of the barrel cortex. J. Neurosci. Methods *263*, 145–154.

Petersen, C.C.H. (2003). The barrel cortex–integrating molecular, cellular and systems physiology. Pflugers Arch. *447*, 126–134.

Petersen, C.C. (2007). The functional organization of the barrel cortex. Neuron *56*, 339–355.

Petersen, C.C.H., and Sakmann, B. (2001). Functionally independent columns of rat somatosensory barrel cortex revealed with voltage-sensitive dye imaging. J. Neurosci. *21*, 8435–8446.

Polley, D.B., Rickert, J.L., and Frostig, R.D. (2005). Whisker-based discrimination of object orientation determined with a rapid training paradigm. Neurobiol. Learn. Mem. *83*, 134–142.

Rothschild, G., and Mizrahi, A. (2015). Global order and local disorder in brain maps. Annu. Rev. Neurosci. *38*, 247–268.

Shimegi, S., Ichikawa, T., Akasaki, T., and Sato, H. (1999). Temporal characteristics of response integration evoked by multiple whisker stimulations in the barrel cortex of rats. J. Neurosci. *19*, 10164–10175.

Shimegi, S., Akasaki, T., Ichikawa, T., and Sato, H. (2000). Physiological and anatomical organization of multiwhisker response interactions in the barrel cortex of rats. J. Neurosci. *20*, 6241–6248.

Simons, D.J. (1978). Response properties of vibrissa units in rat SI somatosensory neocortex. J. Neurophysiol. *41*, 798–820.

Simons, D.J. (1985). Temporal and spatial integration in the rat SI vibrissa cortex. J. Neurophysiol. *54*, 615–635.

Simons, D.J., and Carvell, G.E. (1989). Thalamocortical response transformation in the rat vibrissa/barrel system. J. Neurophysiol. *61*, 311–330.

Thivierge, J.-P., and Marcus, G.F. (2007). The topographic brain: from neural connectivity to cognition. Trends Neurosci. *30*, 251–259.

Wilson, S.P., Law, J.S., Mitchinson, B., Prescott, T.J., and Bednar, J.A. (2010). Modeling the emergence of whisker direction maps in rat barrel cortex. PLoS ONE *5*, e8778.

Woolsey, T.A., and Van der Loos, H. (1970). The structural organization of layer IV in the somatosensory region (SI) of mouse cerebral cortex. The description of a cortical field composed of discrete cytoarchitectonic units. Brain Res. *17*, 205–242.

Zhu, J.J., and Connors, B.W. (1999). Intrinsic firing patterns and whisker-evoked synaptic responses of neurons in the rat barrel cortex. J. Neurophysiol. *81*, 1171–1183.